# Data processing of overturned reflections

*Zhiming Li*

## INTRODUCTION

Large-angle reflectors can generate both normal reflections from the tops of the reflectors and the overturned reflections from under-sides of the reflectors. Imaging the large-angle reflectors requires special techniques both in the stacking and the migrating of these reflections.

Dip-moveout algorithms can be used in the stacking of normal reflections into sections. Large-angle migration methods, such as the phase-shift algorithm and the LInearly Transformed Wave EQuation (LITWEQ) algorithm (Li, 1984), can be applied to migrations of both the normal and the overturned reflections. However, overturned reflections are rarely identified and interpreted in the seismic exploration industry, because there are several difficulties, other than the difficulties in the recording of overturned reflections, in the identification and the stacking of them into sections for migration.

The overturned reflections are likely to be present in field data when seismic surveys are carried over geological structures that have large-angle of reflectors, such as overthrust faults or salt domes. Migrating the overturned reflections will help us better determine the boundaries of these structures. Migration of the overturned reflections can be done with several migration algorithms: 1. Claerbout's two-pass phase-shift depth extrapolation (Li et al, 1984); 2. Reverse-time migration (Baysal et al., 1984); 3. The LITWEQ migration (Li, 1984).

It has been shown in another paper of this report (Li, 1985) that the overturned reflections have negative moveouts in the common midpoint (CMP) gathers. Therefore, negative moveout stacking can stack the overturned reflections into the sections. However, the data aliasing effect due to insufficient sampling in CMP gathers can make the stacking difficult.

The aliasing effect can be avoided or reduced if we do slant stacking in common shot gathers, because the trace interval is usually smaller in the common shot gather than in the CMP gather. The overturned reflections and the normal reflections (reflections from the tops of reflectors) have opposite curvatures in the shot gather (Li, 1985). Therefore, over a certain range of the offsets, the two reflections have different slopes and can be stacked into different sections according to their slopes.

## IDENTIFYING AND STACKING THE OVERTURNED REFLECTIONS

### Overturned reflections

The processing of data with overturned reflections becomes important when we want to accurately determine positions of steeply dipping reflectors, because it can offer another image of under-sides of reflectors. This processing is particularly important in the determining of the boundaries of salt domes. When a seismic survey is carried over a mushroom-shaped salt dome, as shown in Figure 1, it is observed that the normal reflection from one flank of the salt dome is too weak, or incoherent, to be recorded. The reasons for this weakness might be that the incident energy is trapped inside the salt dome because of the high reflectivity on the salt dome boundary, and that the normal reflections are highly attenuated and diffracted by the normal fault systems usually developed over the top of the salt dome. Therefore, the flanks of the mushroom-shaped salt domes are usually missing from the conventional migrated section. On the other hand, the overturned reflection might be recorded because its raypath is completely outside the salt dome. Thus, processing the overturned reflection helps us to locate the flanks of the salt dome.

Processing the overturned reflections has other purposes: 1. A comparison of the normal reflection image and the overturned reflection image can more accurately determine the locations of the dipping reflectors and the velocity distributions; 2. Combining these two images will enhance the resolution of the dipping reflectors.

### Slant stacking

Over a small window on a shot gather, reflection curves can be approximated by certain line segments having the same slopes, $dt/dx$, as those of the original hyperbolas. Figure 2 shows the 16 nearest-offset traces of a gather taken

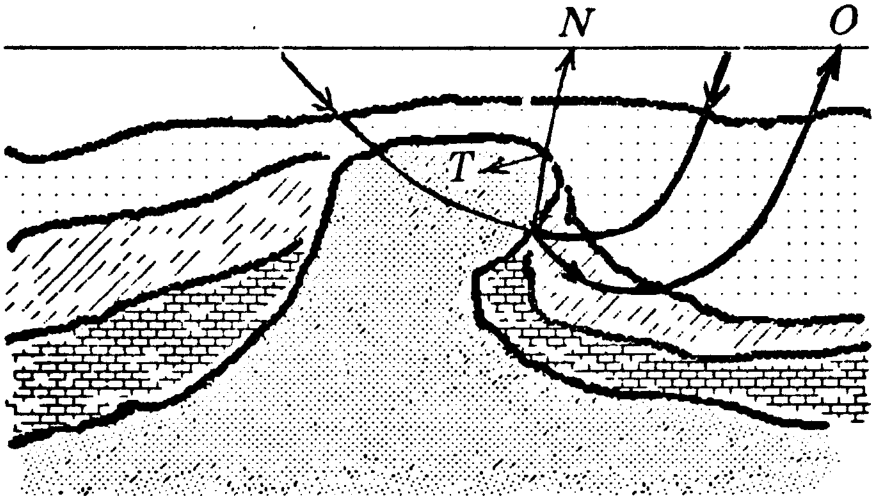

FIG. 1. Normal and overturned reflections over a salt dome. The normal reflection, N, is too weak to be recorded, because part of the energy, T, is trapped inside the salt dome. The overturned reflection, O, is recorded.

from a Chevron dataset in the Gulf of Mexico. In the figure, all the reflections appear as approximately straight line segments.

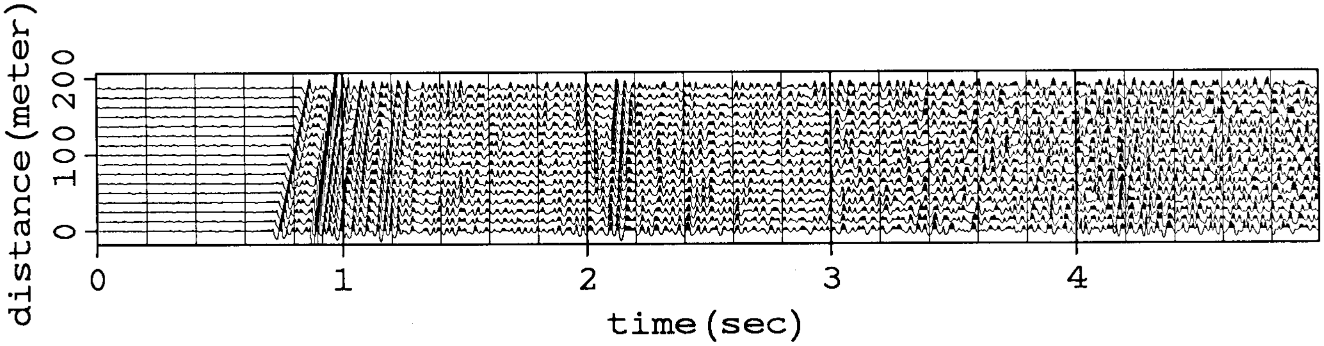

FIG. 2. The 16 nearest-offset traces of a gather from the GASTI line in the Gulf of Mexico. The line crosses over a salt dome.

A few near traces from each shot gather were chosen to be slant stacked. The stacking window is put over the nearest traces of a shot gather for two reasons. First, the geometry of the near-offset trace is close to the zero-offset geometry. It is easier to identify and analyze the overturned reflections in the zero-offset sections than in the non-zero offset sections. Second, the difference between the slopes of a normal reflection and an overturned reflection is larger over the nearer traces (Li, 1985).

Slant stacking with a given slope over this small window will give a trace in which the reflections having this slope are stacked. Equation (1) is the slant stacking formula.

$$S(\tau,p) = \sum_{i=1}^{N} W(x_i)\, P(x_i, \tau + px_i)\,, \tag{1}$$

where $S$ is the stacked trace, $P$ the input trace, $W$ the weighting function, $\tau$ the two-way vertical travel time, $p$ the stacking slope, and $x_i$ the offset of trace i. The stacking is performed over the window that contains $N$ traces.

Continuing this process to all the shots of the line gives a stacked section. Changing the stacking slope, $p$, will give another section on which the group of reflections having this new slope is stacked.

Because the slopes of reflections from flat layers are nearly zero at near traces, the flat layer reflections will be well stacked into the section if the stacking slope is chosen to be zero. A zero-slope stacked section can give us more information about structures under the survey line than other sections stacked with non-zero slopes. Therefore, this section can be used as an guide for our choice of the special stacking slopes for the reflections of interest, such as normal reflections and overturned reflections from some steeply dipping reflectors. Figure 3 shows the zero-slope stacked section of the GASTI line in the Gulf of Mexico. Most of the structures, such as a salt dome and some faults, can be seen in the figure.

Figures 4(a) and 4(b) show the sections stacked with two different stacking slopes.

Stacking again along $p$ axis will give us a **double slant stacking** section as shown in Figure 5. It is clear that both dipping reflections and flat reflections are well stacked into the section, which accomplishes the job of both dip moveout and the normal moveout stacking.

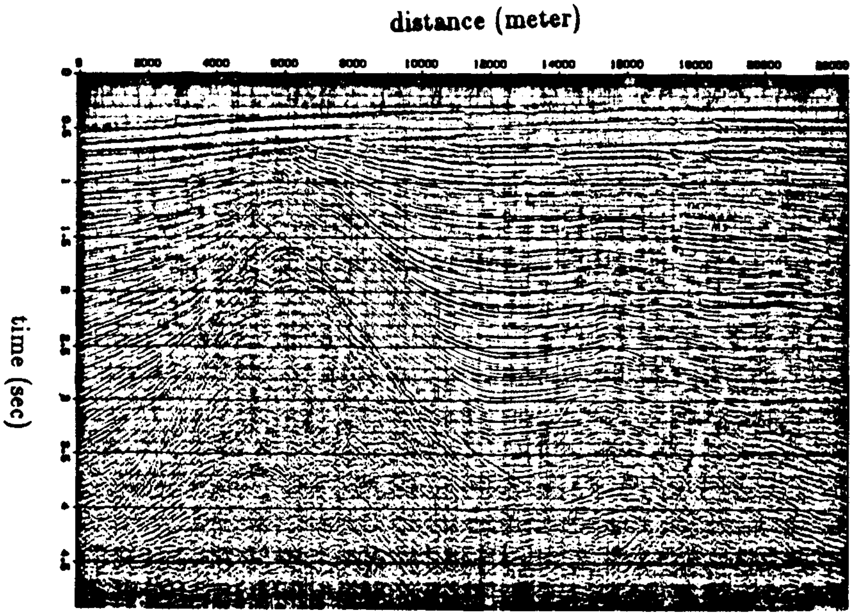

FIG. 3. A slant stacked section of the GASTI line. The slant stacking slope is 0 sec/km, i.e., horizontal. The reflections from the flat layers are well stacked into the section, with this slope.

Some weighting function over the window must be used so that the truncation effect is reduced. The Gaussian function is the weighting in the stackings which have been shown.

The results of slant stacking and other processing of the GASTI line show no convincing indication of the overturned reflections. Overturned reflections travel a long distance before they reach the surface. Therefore, the distance from the reflector to the receiver must be long enough that the overturned reflections are recorded. Because the GASTI line starts close to the possible flank of the mushroom-shaped salt dome, the recording distance might not be long enough for the recording of the overturned reflections from the flank. Another reason for the overturned reflections not appearing in the line is that the recording time length is 5 seconds, this might be too short for the recording of overturned reflections, which might have arrived later.

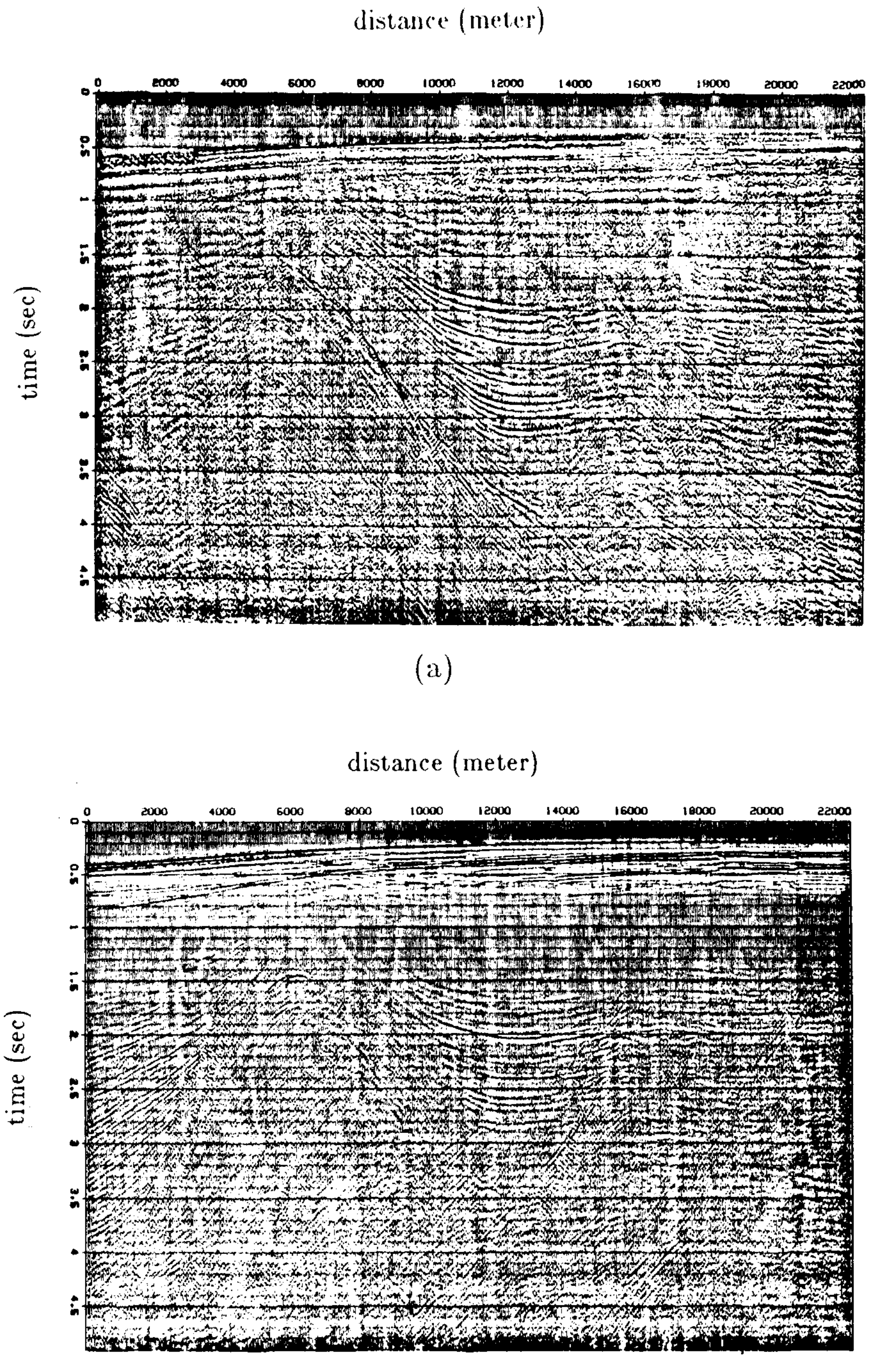

(a)

(b)

FIG. 4. (a) A section of the GASTI line stacked with the slant stacking slope of -1/3 sec/km. The reflections dipping downwards to the right with this slope are stacked into the section. (b) A section of the GASTI line stacked with the slant stacking slope of +1/3 sec/km. The reflections dipping downwards to the left with this slope are stacked into the section.

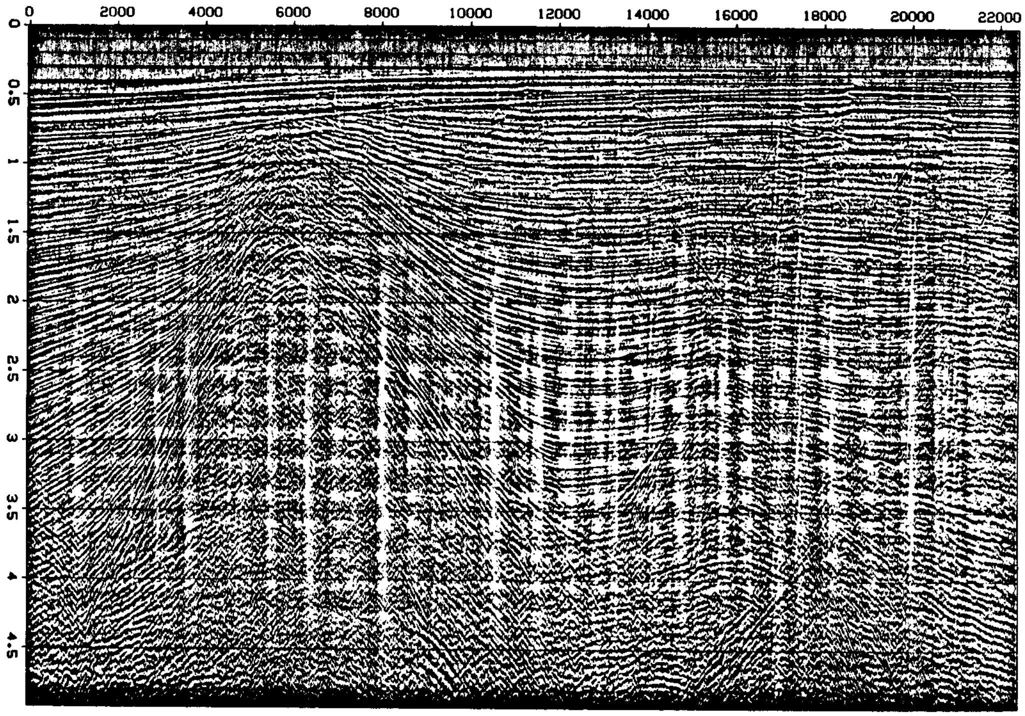

FIG. 5. Double slant stacking section (An approximation to the zero-offset section).

Although no satisfactory results have been obtained from the GASTI line yet, the work on this dataset did give us some useful experiences that might be very beneficial to future research on the other datasets. These prospective datasets should have the following properties: 1. long recording time and long recording cable length; 2. small geophone spacing to reduce aliasing effect; 3. high signal-to-noise ratio, especially at later arrivals of the records.

## MIGRATING OVERTURNED REFLECTIONS IN MEDIA WITH LATERALLY VARYING VELOCITY

Migrating the overturned reflections is easier than identifying and stacking them. Claerbout's two-pass phase-shift depth migration was already described in SEP-38 (Li et al, 1984).

This phase-shift migration is not valid when the velocity is varying laterally. Migration has to be carried out in the physical domain $(t, x, z)$. However, the conventional migration methods, based on different order approximations of the wave equation, have in common the constrains of not being able to migrate the large angle reflections exactly. To preserve the accuracy of migration, the LInearly Transformed Wave EQuation (LITWEQ) method (Li, 1984) was developed at SEP. This new migration method has the economy of the conventional finite difference migration methods, yet requires no approximations as to the dips of the seismic reflections. One of the applications of the LITWEQ is the migration of overturned reflections.

The two-way property and the high accuracy of the LITWEQ make the LITWEQ migration of overturned waves possible. However, the LITWEQ can only offer one image, because both the normal and overturned reflections are migrated simultaneously and merged together when they are imaged at the reflector position. Therefore, the overturned reflection and normal reflection must be separated before the LITWEQ migration is applied, if two images are required. Figure 6 shows that the LITWEQ can migrate both the normal reflection and the overturned reflection, if they are separated before migration.

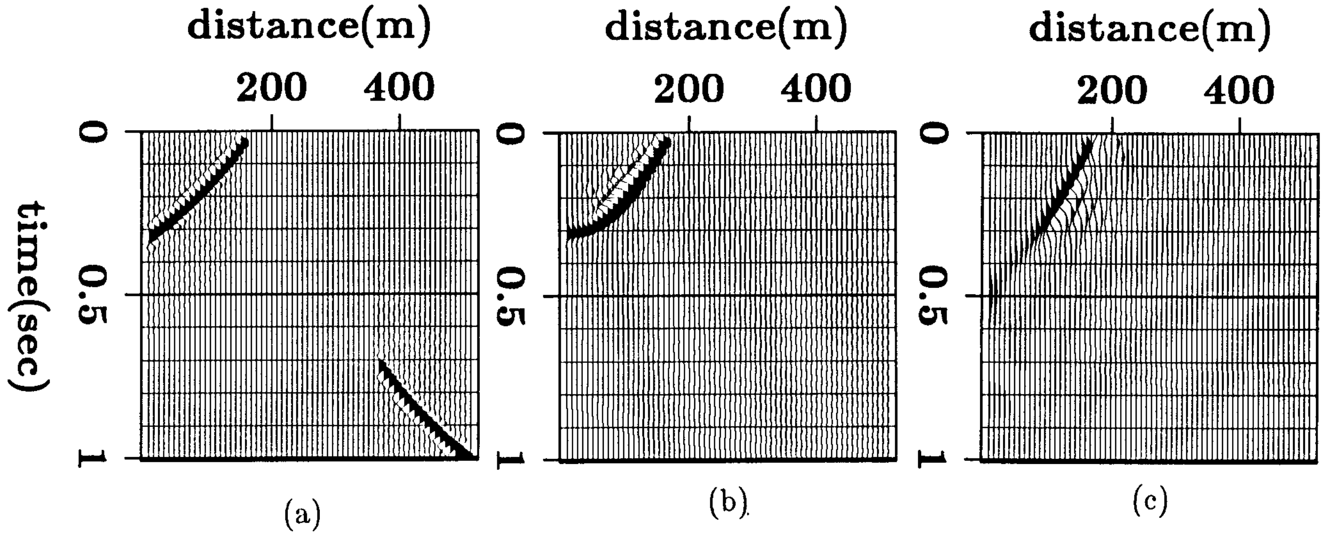

FIG. 6. (a)The stacked section. Normal reflection is on the left upper conner of the panel while overturned reflection present at lower right corner. (b) The LITWEQ migrated section of the upper left event in (a). (c) The LITWEQ migrated section of the lower right event in (a).

## SUMMARY

The algorithms for migrating overturned data have been developed. The major future work is the identification and the stacking of the overturned reflections by either the slant stacking method in the common-shot gather or the moveout stacking method in the common-midpoint gather.

## ACKNOWLEDGMENTS

I would like to thank Jon Claerbout, Richard Ottolini and Chuck Sword for their helpful suggestions and discussions with me on the slant stacking method. Jon Claerbout suggested slant stacking over near traces to get all possible reflections. Thanks are also due to Stewart Levin and Shuki Ronen. I also would like to thank Don Riley of Chevron and Samuel H. Gray of Amoco for their sending us some datasets that I am still working on.

## REFERENCES

Baysal,E., Kosloff,D.D., and Sherwood,J.W.C., 1894, A two-way nonreflecting wave equation: Geophysics, v.49, p.132-141.

Claerbout, J.F., 1985, Imaging the earth's interior: Blackwell Scientific Publications.

Li, Z., Ottolini, R., and Claerbout, J., 1984, Migrating reflections greater than 90 degrees via depth extrapolation: SEG Expanded Abstracts with Biographies of 1984 Technical Program, p.696-700.

Li, Z., 1984, Wave field extrapolation by the linearly transformed wave equation operator, SEP-41, pp 167-189.

Li, Z., 1985, Seismic modeling in medium with linear velocity gradient: SEP-42.

# STANFORD UNIVERSITY

▬ **Free TIME LIMIT Parking**
8 to 5, Monday through Friday

▨ **PAY LOT and/or METER Parking**
(coins needed except at Medical Center)
8 to 5, Monday through Friday

● **HANDICAP Parking** ♿
For use **only** by persons with handicap parking permits. Enforced at all hours every day. **$52 minimum fine** for parking in these zones without proper permit.

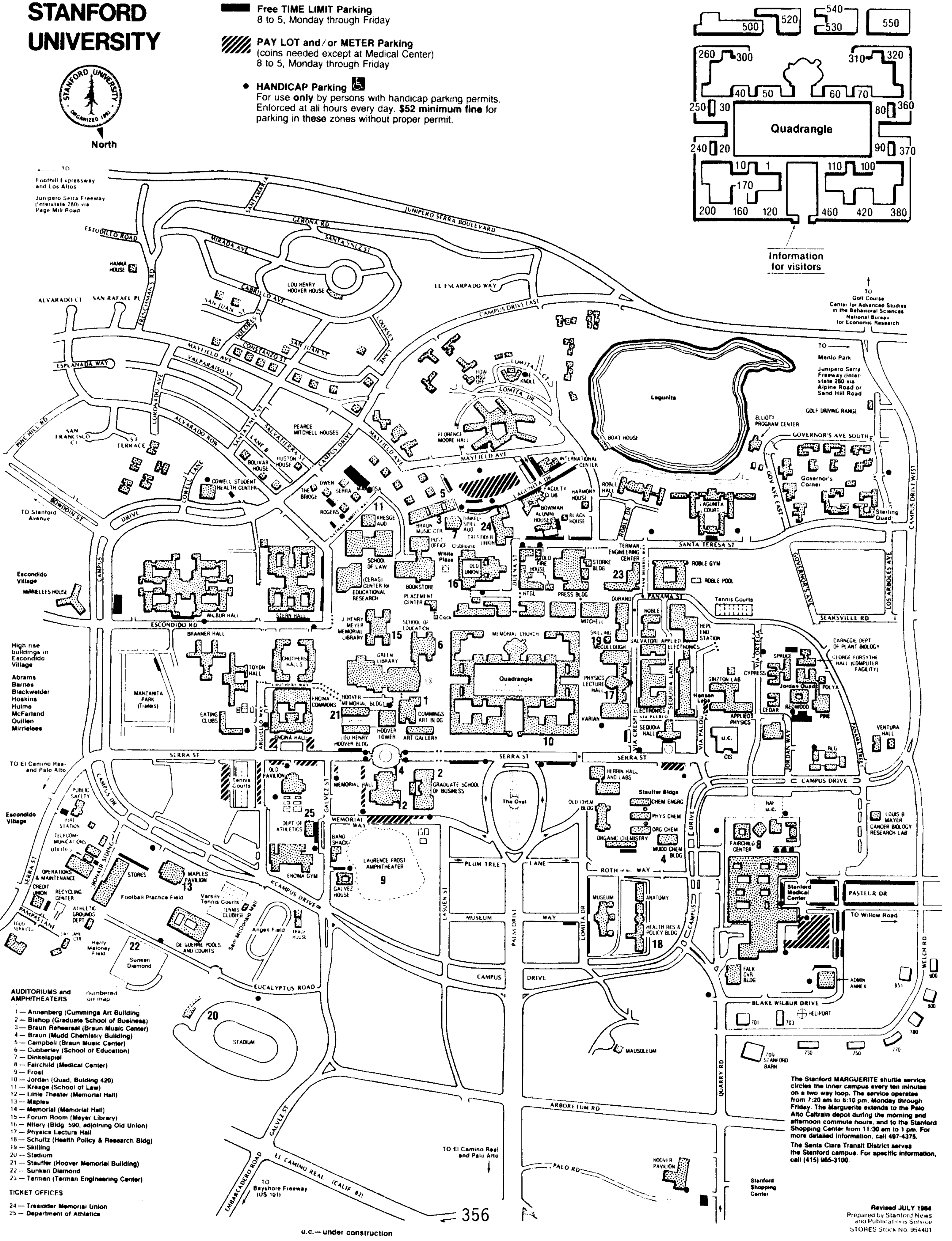

**AUDITORIUMS and AMPHITHEATERS** numbered on map

1 — **Annenberg (Cummings Art Building**
2 — **Bishop (Graduate School of Business)**
3 — **Braun Rehearsal (Braun Music Center)**
4 — **Braun (Mudd Chemistry Building)**
5 — **Campbell (Braun Music Center)**
6 — **Cubberley (School of Education)**
7 — **Dinkelspiel**
8 — **Fairchild (Medical Center)**
9 — **Frost**
10 — **Jordan (Quad, Building 420)**
11 — **Kresge (School of Law)**
12 — **Little Theater (Memorial Hall)**
13 — **Maples**
14 — **Memorial (Memorial Hall)**
15 — **Forum Room (Meyer Library)**
16 — **Nitery (Bldg. 590, adjoining Old Union)**
17 — **Physics Lecture Hall**
18 — **Schultz (Health Policy & Research Bldg)**
19 — **Skilling**
20 — **Stadium**
21 — **Stauffer (Hoover Memorial Building)**
22 — **Sunken Diamond**
23 — **Terman (Terman Engineering Center)**

TICKET OFFICES

24 — **Tresidder Memorial Union**
25 — **Department of Athletics**

**The Stanford MARGUERITE shuttle service circles the inner campus every ten minutes on a two way loop. The service operates from 7:20 am to 6:10 pm, Monday through Friday. The Marguerite extends to the Palo Alto Caltrain depot during the morning and afternoon commute hours, and to the Stanford Shopping Center from 11:30 am to 1 pm. For more detailed information, call 497-4375.**

**The Santa Clara Transit District serves the Stanford campus. For specific information, call (415) 965-3100.**

u.c.—under construction

**Revised JULY 1984**
Prepared by Stanford News
and Publications Service
STORES Stock No. 954401